The Influence of Fe and Cr on the Microstructure of Cast Al-Si-Mg Alloys

G. GUSTAFSSON, T. THORVALDSSON, and G. L. DUNLOP

The detailed microstructure of cast aluminum alloys based on Al-7 pct Si-0.3 pct Mg (A356) has been investigated as a function of Fe and Cr content and solidification rate. It was found that the coarse β phase ($FeSiAl_5$) platelets, which form during solidification of alloys containing Fe, are replaced by "Chinese script" α(bcc) [$(Cr,Fe)_4Si_4Al_{13}$] dendritic particles when Cr is added. Coarse π ($FeMg_3Si_6Al_8$) phase and fine α(bcc) precipitates were found in all of the investigated alloys. Quantitative metallography showed that the length of β phase platelets and the arm length of α(bcc) dendrites increased with decreasing solidification rate and increased Fe content. The T6 heat treatment resulted in the dissolution of π phase and the uniform fine scale precipitation of $\beta'(Mg_2Si)$ in the aluminum rich phase.

I. INTRODUCTION

CAST aluminum alloys of the type A356 (Al-7 pct Si-0.3 Mg) have widespread applications, especially in the automotive and aircraft industries. Increasing demands on such material properties as tensile strength, ductility, and corrosion behavior have pointed to the need for close microstructural control through tighter specification of composition, casting practice, and subsequent heat treatment.

One of the most important parameters in determining the properties of these alloys is the rate of solidification. This determines the coarseness of the microstructure and the amount of porosity. Increased solidification rates result in finer microstructures and improved mechanical properties.[1,2]

Iron is the most deleterious impurity element in cast aluminum alloys since, as shown in Figure 1 for the ternary Al-Fe-Si system, intermetallic phases such as α (Fe_2SiAl_8) and β ($FeSiAl_5$) form during solidification. Of these intermetallic phases β in particular is considered to be detrimental for the ductility of the material. It has been shown previously that the size and amount of iron-containing phases is strongly influenced by solidification rate[5,6,7] and that alloying elements such as Mn, Cr, Ni, and Co can change the morphology of the intermetallic phases or enhance the precipitation of phases which are less harmful than β.[6,8]

Mn is the most common alloying addition which is used to modify the morphology and type of intermetallic phases in cast aluminum alloys. It has been reported that additions of Cr can have a similar effect,[3] but the microstructural details are not clear. In the present investigation the influence of Cr additions on microstructure has been studied as a function of solidification rate in Al-7 pct Si-0.3 pct Mg alloys containing 0.2 pct and 0.5 pct Fe. These iron contents are typical of alloys prepared from primary aluminum and remelt aluminum ingots, respectively.

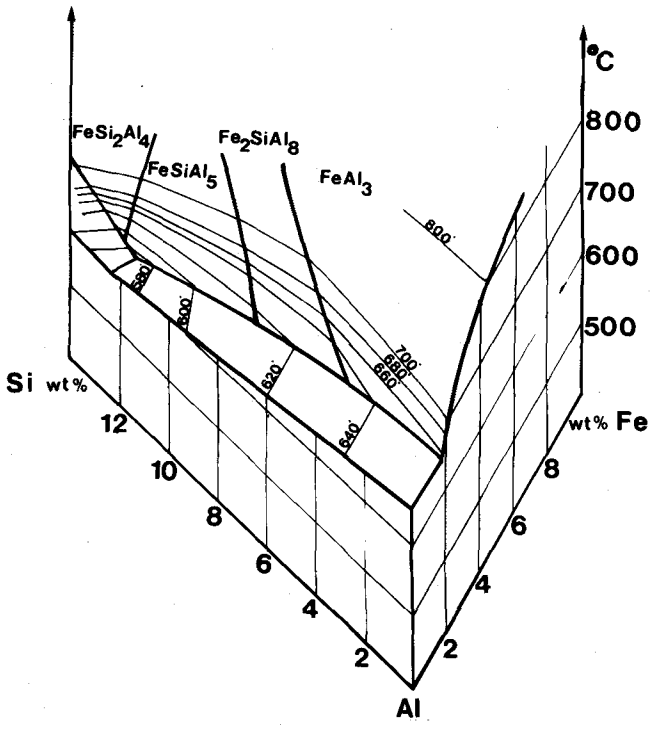

Fig. 1 — Liquidus surfaces in the Al-rich corner of the Al-Fe-Si equilibrium phase diagram. Based on data from Mondolfo[3] and Rivlin and Raynor.[4]

The microstructural investigation was carried out by a combination of optical metallography, electron probe microanalysis (EPMA), scanning electron microscopy (SEM), and analytical transmission electron microscopy (TEM/STEM/EDX). The detailed microstructure of cast aluminum alloys as elucidated by transmission electron microscopy (TEM) has received only a little attention previously,[9,10] and therefore some emphasis has been placed on this aspect in the present work.

II. EXPERIMENTAL

The investigation was conducted on four alloys with compositions as given in Table I. The base alloy, Alloy 1, is of type A356. Alloys 3 and 4 have a higher Fe content, and Alloys 2 and 4 have similar Cr additions to the Fe contents.

G. GUSTAFSSON, formerly with Chalmers University of Technology, Göteborg, Sweden, is now with Laboratory for Metallic Materials AB Volvo, Göteborg, Sweden. T. THORVALDSSON is Physical Metallurgist at R and D Center of AB Sandvik Steel, Sandviken, Sweden. G. L. DUNLOP is with the Department of Physics, Chalmers University of Technology, Göteborg, Sweden.

Manuscript submitted September 12, 1984.

Table I. Chemical Compositions of the Experimental Alloys (Wt Pct)

Alloy	Fe	Cr	Si	Mg	Sr	Cu	Mn, Zn, Ni, Sn, Ti, Ca
1	0.20	0.002	6.8	0.36	0.030	0.001	<0.010
2	0.20	0.20	6.6	0.31	0.021	0.001	<0.010
3	0.52	0.002	6.6	0.30	0.019	0.025	<0.010
4	0.50	0.37	6.6	0.29	0.019	0.025	<0.010

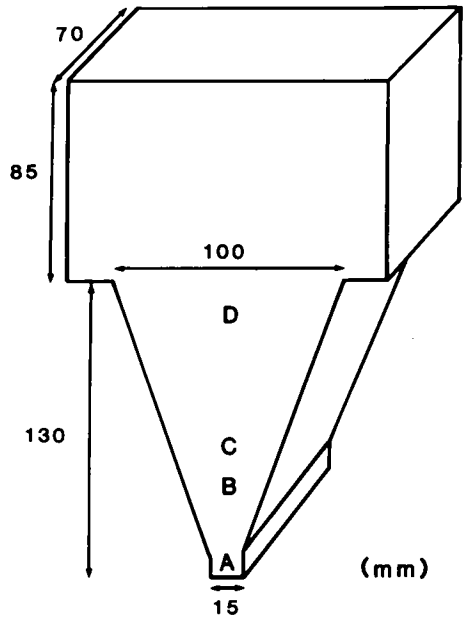

Fig. 2—The wedge-shaped mold. Specimen positions A-D for subsequent metallography are indicated.

The melts were poured at a temperature of 720 °C into a wedge-shaped permanent mold (Figure 2) in order to produce a range of solidification rates within the same ingot. Specimens for microstructural investigation were taken from the positions A-D indicated in Figure 2. The samples that were given the T6 heat treatment were treated in the following way:

(i) solution treatment at 520 °C for 4 hours;
(ii) quenching into hot water at 80 °C;
(iii) holding at room temperature for times longer than 24 hours;
(iv) aging at 170 °C for 10 hours;
(v) air cooling.

Specimens for optical metallography were mechanically polished and etched in 20 pct H_2SO_4 for 20 seconds at 70 °C. This etchant attacks the β phase preferentially. Secondary dendrite arm spacings (DAS) and size distributions of intermetallic phases were determined by intercept measurements.

Specimens for transmission electron microscopy were prepared by jet polishing in an electrolyte consisting of 30 pct HNO_3 in methanol at 20 V and room temperature. They were then examined using a JEOL 200 CX TEM/STEM electron microscope equipped with a Link Systems energy dispersive X-ray (EDX) spectrometer. Quantitative EDX results were obtained at an accelerating voltage of 200 kV using the Link Systems RTS-2/FLS computer program which compares peak shapes with stored standard spectra, uses a peak stripping routine, applies the Cliff-Lorimer[11] thin foil approximation with experimentally determined k_{XSi} values for light elements,[12] and corrects for absorption.[13]

Electron microprobe measurements were performed on polished bulk specimens at an accelerating voltage of 15 kV using a JEOL Superprobe 733.

III. RESULTS

A. *General Microstructure*

The microstructure of all alloys was dominated by aluminum dendrites which were surrounded by a modified eutectic mixture of a continuous aluminum phase and silicon particles. As shown in Figure 3, the coarseness of the microstructure varied inversely with solidification rate. In order to determine the solidification rate for the four specimen positions in the block, the secondary dendrite arm spacing (DAS) was measured.[14] The solidification rate was calculated according to:[15]

$$\log\left(\frac{dT}{dt}\right) = -\left(\frac{\log(\mathrm{DAS}) - 1.66}{0.40}\right)$$

where dT/dt is given in °C per second and DAS in μm. The results of the DAS measurements and calculated solidification rates are given in Table II. No significant variation among the four alloys was noted in DAS measurements made at equivalent positions in the ingots. It can be noted that there was a difference of two orders of magnitude in solidification rate between positions A and D in the castings.

Optical micrographs taken at position B in the castings for all four alloys are shown for comparison in Figure 4. It can be noted that the solidification rate associated with this position is similar to the average rate which is experienced in production of permanent mold castings of such components as car wheels.

For all four alloys the eutectic was usually modified by the strontium addition[16,17] (see Table I). However, at the slowest solidification rate (position D in Figure 3) the strontium addition was not sufficient for complete modification of the eutectic, and the silicon phase was very plate-like. At this slow solidification rate some large inclusions (~10 μm in size; see Figure 5) of a phase containing significant quantities of Al, Si, Ca, and Sr were found by EDX analysis and scanning electron microscopy. It would thus seem that the formation of this Sr-containing phase at an early stage of solidification is responsible for the poor modification at slow solidification rates.

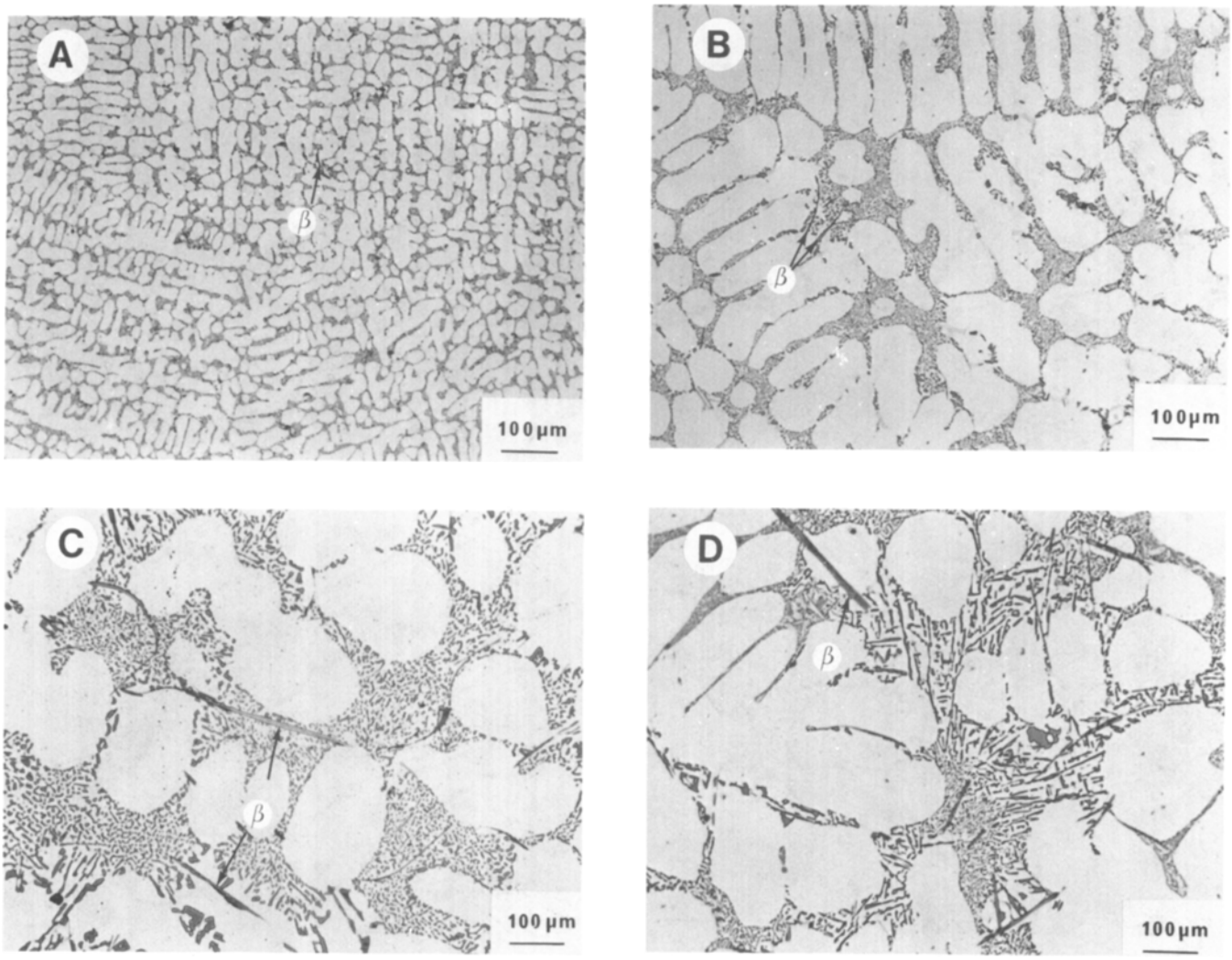

Fig. 3 — As-cast microstructure of Alloy 3 at positions A-D showing aluminum dendrites in a modified eutectic of Al and Si. β ($FeSiAi_5$) platelets are indicated.

Table II. Measured Secondary Dendrite Arm Spacing (DAS) and Calculated Solidification Rates at the Positions Given in Figure 2

		A	B	C	D
DAS	(μm)	15	35	50	90
Solidification rate	(°C/s)	16	1.9	0.8	0.2

B. *Coarse Intermetallic Phases*

The coarse intermetallic phases which were identified by a combination of morphology, electron probe microanalysis, and etching characteristics[7] (see Table III) are indicated in Figures 4 and 6.

Both β and π phases were present in the as-cast condition of the alloys which did not contain Cr (*i.e.*, Alloys 1 and 3). The β phase formed as large platelets, and π phase often nucleated on the β platelets (see Figure 6). The intermetallic phases in the Cr-containing alloys (Alloys 2 and 4) were α(bcc) and π. The α(bcc) phase generally has a dendritic morphology which appears as "Chinese script" in polished sections. A good understanding of the morphology of both β and α(bcc) phases can be obtained by the SEM micrographs of deep etched sections shown in Figure 7.

Results of electron microprobe measurements made on coarse intermetallic phases from position B in all four alloys are given in Table IV. It is possible that some of the aluminum matrix was included in the volumes which were analyzed, and therefore the concentration ratio (Cr + Fe)/Si is used as a suitable parameter to distinguish the phases. The error limits which are quoted for this ratio are the standard deviations from a number of measurements. The (Cr + Fe)/Si value for β phase was approximately 1 with a fairly large standard deviation for as-cast Alloys 1 and 3. This ratio increased to 1.4 with a much lower standard deviation when Alloy 3 was given a T6 temper. The (Cr + Fe)/Si values for π phase were consistent at 0.3 with generally low standard deviations. For the Cr-containing Alloys 2 and 4 the "Chinese script" α(bcc) phase had (Cr + Fe)/Si ratios which were somewhat greater than 2.

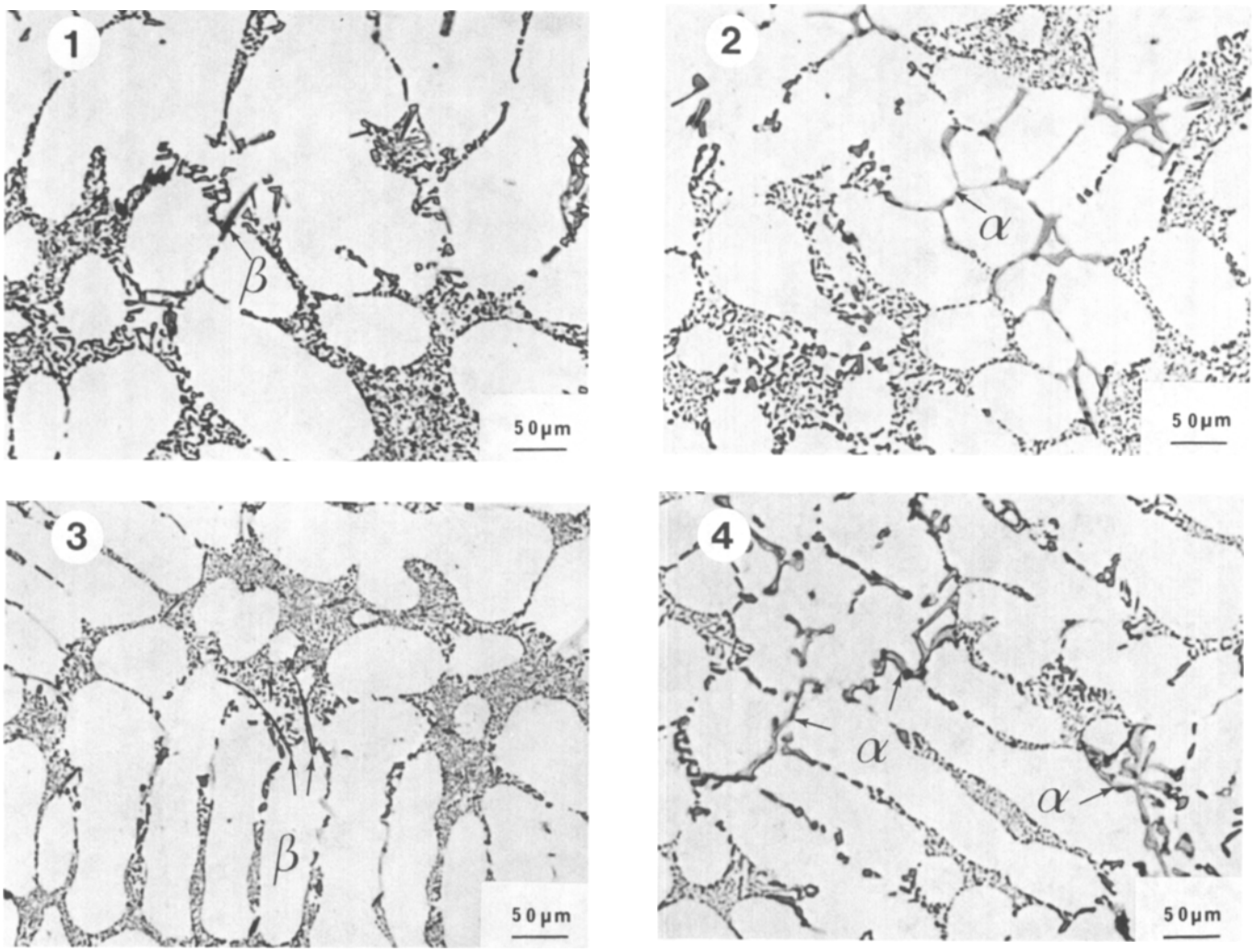

Fig. 4 — As-cast microstructure of Alloys 1-4 at position B (DAS = 35 μm). β ($FeSiAl_5$) and α(bcc) [$(Cr, Fe)_4Si_4Al_{13}$] are indicated.

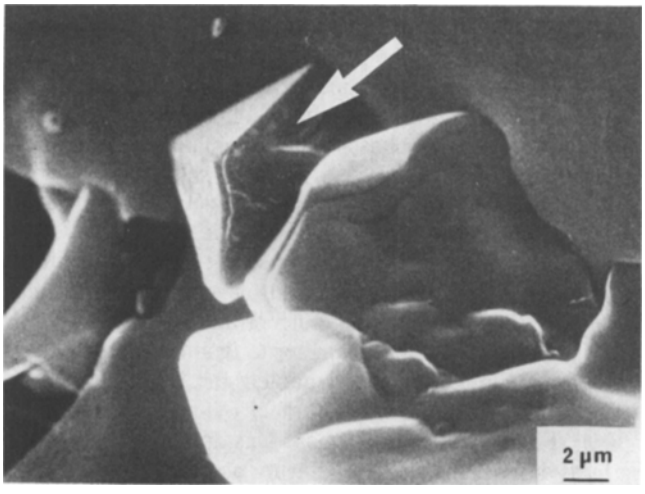

Fig. 5 — Inclusions containing Ca, Sr, Si, and Al in the eutectic of Alloy 2 at position A.

Size measurements were made on α(bcc) and β phases using optical metallography on polished sections. For the β phase the dimension measured was the plate length in the section while for α(bcc) similar measurements were made on the dendrite arms (see Figure 8). For each set of measurements the dimensions were found approximately to follow a normal distribution. As shown in Figure 8 the mean measured particle lengths varied significantly with solidification rate. It can also be seen that the particle lengths were also dependent upon the Fe and Cr content of the alloys. For equivalent Fe-contents the mean phase lengths for α(bcc) and β were similar, but the standard deviation of the measurements was considerably greater for β. This suggests that the maximum β plate length in a certain volume is generally greater than the maximum α(bcc) arm size.

C. *Fine Intermetallic Phases*

In all four alloys fine (0.1 to 1 μm) intermetallic phases were observed in the eutectic by TEM of both the as-cast and

Table III. Structure and Composition of Experimentally Observed Intermetallic Phases (Wt Pct)

phase	structure (3)	Mg	Si	Cr	Fe	(Cr + Fe)/Si	reference
β	monoclinic		12 to 15		25 to 30	2.2	Mondolfo[3]
$FeSiAl_5$	a, b 0.612 nm		13.8 to 14.9		26.7 to 27.3	1.9	Pratt-Raynor[18]
	c 4.15 nm		15.8 to 18.9		23.5 to 25.8	1.4	Obinata-Komatsu[19]
	91 deg		17		29	1.7	Closset-Gruzleski[16]
			18 to 19		16 to 25	1.2	present work, as-cast
			17		24	1.4	present work, T6
π	hcp	15.6	33.8		12.1	0.3	Mondolfo[3]
$FeMg_3Si_6Al_8$	a 0.663 nm	13	28		10	0.3	Closset-Gruzleski[16]
	c 0.794 nm	13 to 16	25 to 28		8 to 9	0.3	present work
α	bcc		6 to 8		(27 to 35)	4.2	Mondolfo[3]
$(Cr,Fe)_4Si_4Al_{13}$	a 1.25 nm		10 to 11	8 to 9	16 to 19	2.2	present work

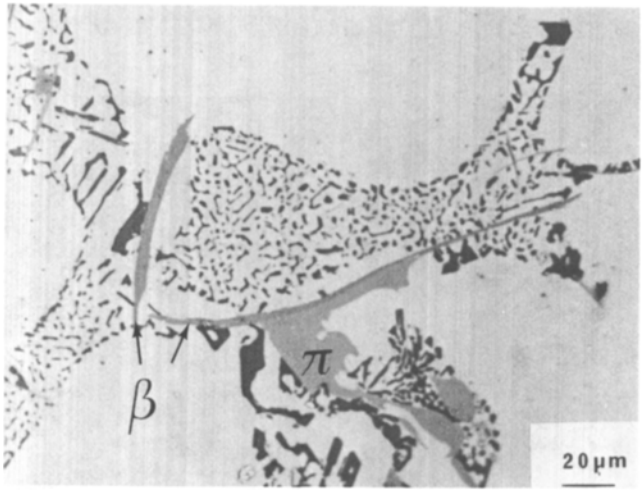

Fig. 6—β ($FeSiAl_5$) and π ($FeMg_3Si_6Al_8$) phases in the as-cast eutectic of Alloy 3 at position D.

T6 conditions (Figure 9). Most of these precipitates could be identified by selected area electron diffraction as the α(bcc) phase which also appears as "Chinese script". The compositions of these precipitates were determined by STEM/EDX. The EDX spectra in Figure 10, which were taken from α(bcc) phase precipitates in as-cast Alloys 3 and 4 at position B, indicate that considerable amounts of Cr can dissolve in this phase. Measured average compositions based on these and other spectra are shown in Table V. Here it can be seen that the (Cr + Fe)/Si ratio for these precipitates increases during the T6 temper.

D. *Microstructural Changes during T6 Temper*

No changes were noted in size, number, or morphology of the α(bcc) and β phases during the T6 heat treatment. However, some compositional changes were noted (see Tables IV and V) indicating that the compositions of these phases were closer to equilibrium after heat treatment. The Mg-containing π phase dissolved during solution treatment and did not reprecipitate. During the heat treatment, Si precipitates approximately 0.5 μm in size appeared in the Al-dendrites of slowly solidified material (positions C and D), but this did not occur in more rapidly solidified material (see Figure 11).

Fine-scale precipitation of intermediate $\beta'(Mg_2Si)$ occurred during the T6 heat treatment in all alloys and for all solidification rates (Figure 12).[20] As in the case of wrought alloys, where this precipitate also appears on heat treatment, the precipitates were rod-like in shape and aligned orthogonally in ⟨100⟩ directions. The precipitate dispersions were similar in both Al-dendrites and eutectic Al, and no differences could be noted between the different alloys and solidification rates.

IV. DISCUSSION

It was found that the types of intermetallic phases which appeared in each alloy were independent of solidification rate in the range investigated (0.2 to 16 °C per second). There was, however, a distinct effect depending on whether Cr was included in the alloy composition. For the two alloys which did not contain Cr the coarse intermetallic phases which appeared on solidification were β and π, while when Cr was present the corresponding phases were α(bcc) and π. Finer scale α(bcc) phase precipitated in the eutectic of all alloys independent of whether Cr was present or not.

The stoichiometry of β phase is usually given as $FeSiAl_5$.[3,4] However, as shown in Table III the composition of this phase can vary considerably depending upon the conditions under which it forms. In the present work, microprobe analysis showed that the composition of the β phase was considerably substoichiometric in the as-cast condition, but came closer to the expected composition during the T6 temper. For this condition, the measured composition of the β phase was the same as that determined by Obinata and Komatsu[19] by chemical analysis of extracted well-formed crystals (see Table III).

The coarse "Chinese script" α(bcc) phase, which replaced the β phase platelets when Cr was present, and also the smaller α(bcc) phase precipitates, which appeared in all four alloys, had compositions which varied widely. No detailed studies of the compositional range of this phase in the Al-Cr-Fe-Si system have been reported previously, but in the Al-Mn-Fe-Si system the related cubic phase can exist over an extremely wide range of compositions.[3,21] It should be noted that in the absence of transition elements other than Fe the coarse α(bcc) phase does not usually form in Al-Fe-Si alloys. However, another more common phase, which is also termed α but which has hexagonal symmetry, may form in such cases.[22]

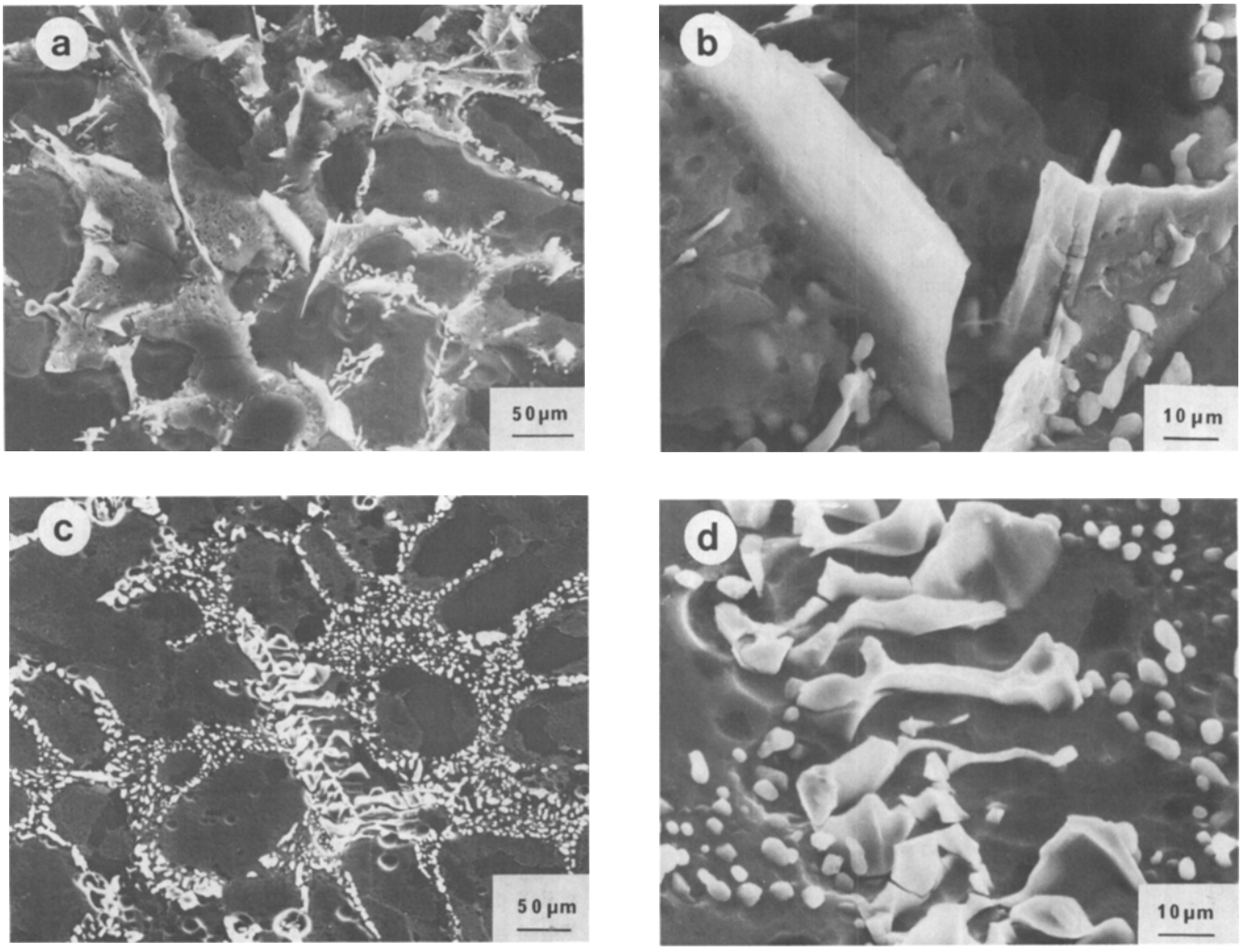

Fig. 7—β and α(bcc) phases revealed by etching in NaOH after T6 heat treatment. (*a*) Alloy 3 position D. β phase with platelet morphology. (*b*) Higher magnification of (a). (*c*) Alloy 4 position D. α(bcc) phase with dendritic morphology. (*d*) Higher magnification of (c).

Table IV. Microprobe Analysis of Intermetallic Phases (Wt Pct) at Position B, DAS = 35 μm

Temper	Alloy	Phase	(Cr + Fe)/Si $\bar{x}$	(Cr + Fe)/Si σ	Mg	Al	Si	Cr	Fe
As-cast	1	β	1.0	±0.2		64	19		16
		π	0.3	±0.01	16	48	28		9
	2	α(bcc)	2.1	±0.2		64	11	8	16
		π	0.3	±0.01	16	47	28		8
	3	β	1.2	±0.3		57	18		25
		π	0.3	±0.1	13	55	25		8
	4	α(bcc)	2.3	±0.3		61	10	9	19
		π	not analyzed						
T6	3	β	1.4	±0.1		60	17		24

In the present study small α(bcc) precipitates formed in all four alloys (see Figure 9). Similar observations have been made previously by Westengen[23] for a direct chilled cast dilute Al-Fe-Si alloy. It would seem that, in such circumstances, the appearance of α(bcc) may be a function of either the nonequilibrium solidification rate or the other elements which may be present as impurities.

The electron microprobe composition measurements of π phase, which was found in the as-cast condition for all four alloys, agree well with previous measurements by Mondolfo[3] and Closset and Gruzleski[16] (see Table III). This phase contains a significant amount of Mg and dissolves during solution treatment. The Mg subsequently precipitates as intermediate $\beta'(Mg_2Si)$ during heat treatment. Thus, the π

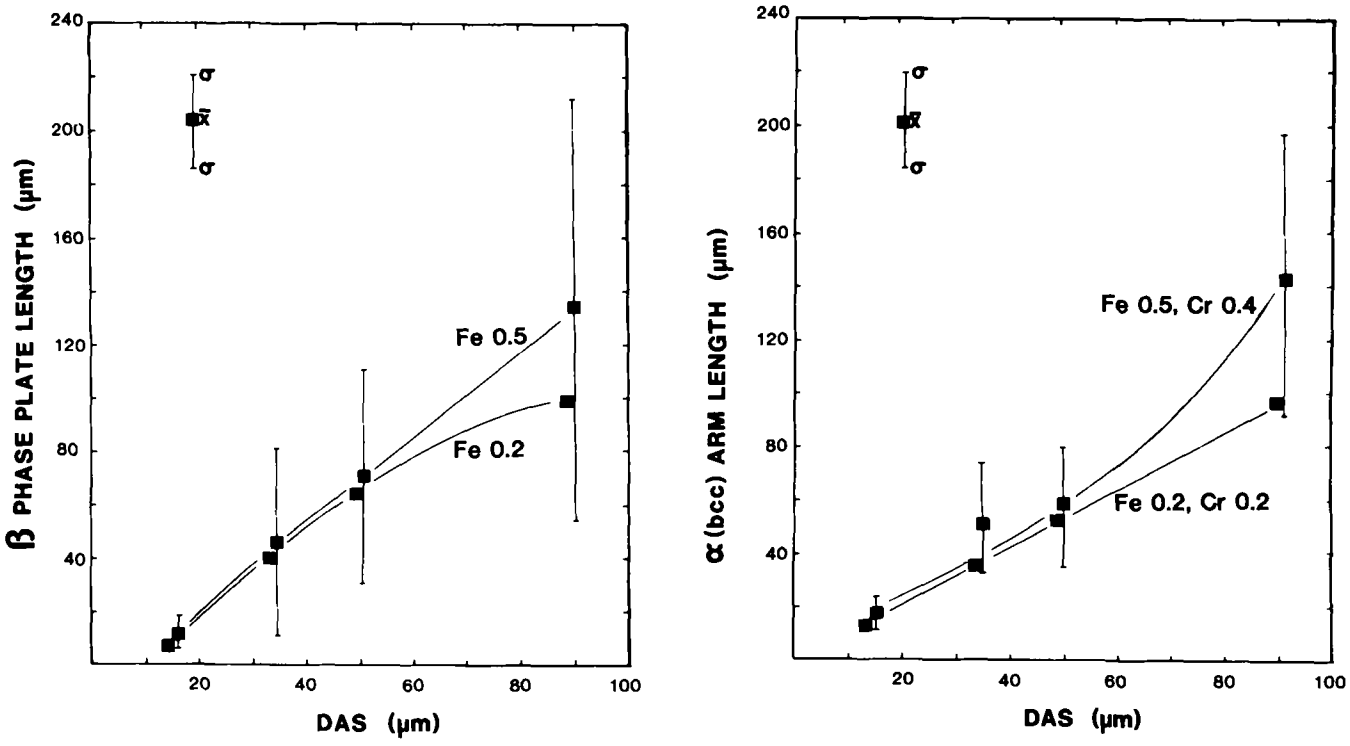

(a) (b)

Fig. 8—Length measurements of β in Alloys 1 and 3 in (*a*) and of α(bcc) in Alloys 2 and 4 in (*b*). The bars indicate the size distribution at a given position. For clarity bars are shown only for the uppermost curves.

Fig. 9—α(bcc) particle in the eutectic of Alloy 1 at position A after T6 heat treatment.

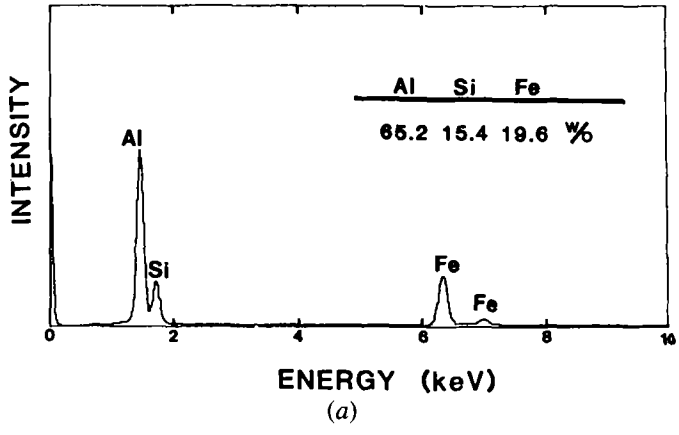

(a)

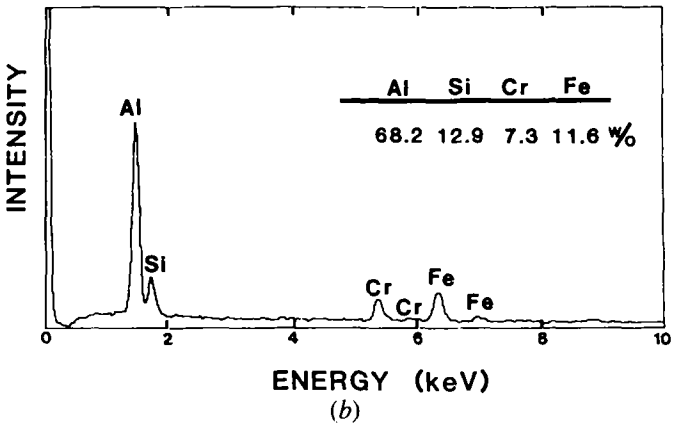

(b)

Fig. 10—EDX spectra of α(bcc) particles. Specimen in the as-cast condition. (*a*) Alloy 3 position B. (*b*) Alloy 4 position B.

phase is not present in the microstructure in the T6 condition. Closset and Gruzleski[16] have shown that for a similar alloy with the higher Mg content of 0.65 pct not all of the π phase is dissolved during solution treatment. The time and temperature of solution treatment for alloys of this type is normally chosen so that π phase can be fully dissolved and also so that the Si phase in the eutectic mixture can spherodize.

During age hardening the intermediate $\beta'(Mg_2Si)$ phase precipitates. It would seem from the present work that neither the Cr nor the Fe content of the alloy nor the solidification rate play any important role in determining the dispersion parameters for this precipitate. Thus it is primarily the Mg content and the conditions (*i.e.*, times and

Table V. Compositions of Fine α(bcc) Precipitates as Determined by STEM/EDX (Wt Pct)

Temper	Alloy and Position	Lattice Parameter (nm)	(Cr + Fe)/Si	Al	Si	Cr	Fe
As-cast	3B	1.25	1.3	64	16		20
	4B	1.24	1.6	64	14	9	13
T6	1A	1.26	2.9	60	10		30
	2A	1.29	2.4	53	15	11	21

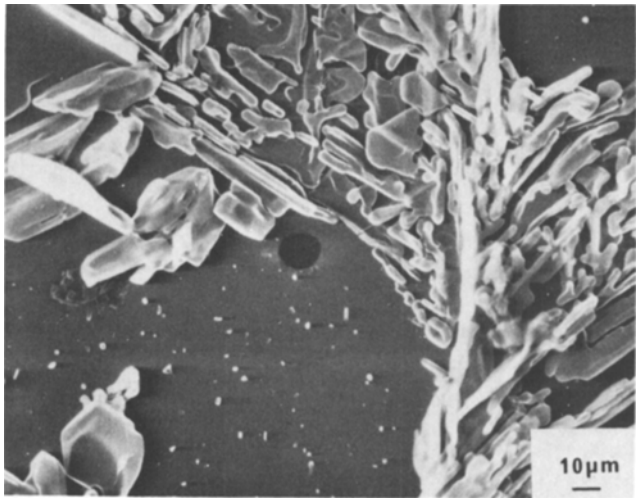

Fig. 11 — Si precipitates in the dendrites of slowly solidified material after T6 heat treatment. Alloy 1 at position D.

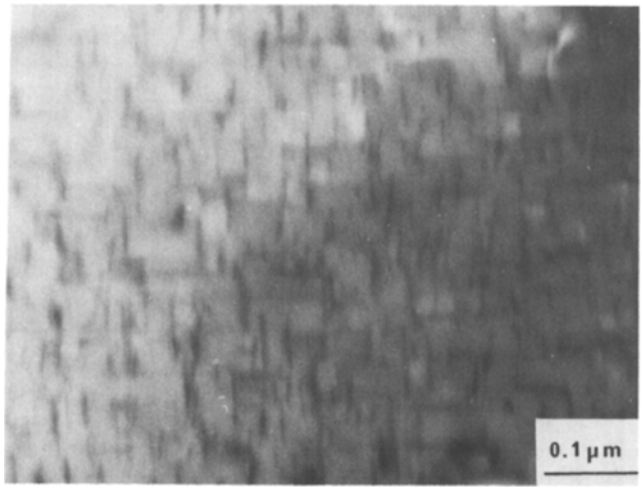

Fig. 12 — Fine $\beta'(Mg_2Si)$ precipitation in a dendrite of Alloy 1 at position A after T6 heat treatment.

temperatures) of the T6 heat treatment which determines the nature of this fine precipitate.

It would seem from the present work that Cr additions have a similar effect to that which is well established for additions of Mn to casting alloys of this type. It is usual practice to balance the Fe content of remelt casting alloys with Mn additions. This has the effect of replacing much of the harmful plate-shaped β intermetallic phase by "Chinese script" phase with a subsequent improvement in tensile ductility and fracture toughness. The present work indicates that the microstructural process which is responsible for these improvements may possibly be even more effective when Cr is used instead of Mn.

V. CONCLUSIONS

1. The as-cast microstructure of the alloys consisted of Al dendrites, a modified eutectic, and intermetallic phases.
2. Additions of Cr resulted in the formation of the coarse "Chinese script" α(bcc) intermetallic phase during solidification instead of plate-shaped β phase particles. Coarse π phase and fine α(bcc) formed in all of the investigated alloys.
3. The length of β platelets and arms of α(bcc) phase increased with decreasing solidification rate and increasing Fe content.
4. The T6 heat treatment results in the dissolution of π phase and the uniform fine scale precipitation of β' (Mg_2Si) in both dendritic and eutectic Al.

ACKNOWLEDGMENTS

The assistance of J. D. Evensen of Årdal og Sunndal Verk in casting the material is greatly appreciated as is the financial support of the Swedish Board for Technical Development.

REFERENCES

1. A. Wickberg, G. Gustafsson, and L-E. Larsson: *SAE Tech. Paper Ser.*, 1984, 840121.
2. K. J. Oswalt and M. S. Misra: *AFS Int. Cast. Met. J.*, 1981, vol. 6, p. 23.
3. L. F. Mondolfo: *Aluminum Alloys, Structure and Properties*, Butterworths, London, 1976.
4. V. G. Rivlin and G. V. Raynor: *Int. Met. Rev.*, 1981, vol. 26, p. 133.
5. J. D. Evensen and T. B. Pedersen: *Proc. 7th Int. Light Met. Conf.*, 1981, Leoben/Vienna, p. 77.
6. A. Couture: *AFS Int. Cast. Met. J.*, 1981, vol. 6, p. 9.
7. G. Phragmén: *J. Inst. Met.*, 1950, vol. 77, p. 489.
8. J. Iglessis *et al.*: *Mém. Sci. Rev. Métall.*, 1977, vol. 73, p. 237.
9. M. S. Misra and K. J. Oswalt: *AFS Trans.*, 1982, vol. 90, p. 1.
10. M. Kaczorowski *et al.*: *J. Met. Sci.*, 1979, vol. 14, p. 2781.
11. G. Cliff and G. W. Lorimer: *J. Microscopy*, 1975, vol. 103, p. 203.
12. G. Wirmark, T. Thorvaldsson, and H. Nordén: *Proc. Inst. Phys. conf. Ser. No. 68*, 1984, ch. 3, p. 71.
13. J. I. Goldstein *et al.*: *Proc. Scanning Electron Microscopy*, IITRI, Chicago, IL, 1977, vol. 1, p. 315.
14. R. E. Spear and G. R. Gardner: *AFS Trans.*, 1963, vol. 71, p. 209.
15. M. Droutzy and M. Richard: *Fonderie*, 1969, vol. 285, p. 500.
16. B. Closset and J. E. Gruzleski: *Metall. Trans. A*, 1982, vol. 13A, p. 945.
17. M. D. Hanna *et al.*: *Metall. Trans. A*, 1984, vol. 15A, p. 459.
18. J. N. Pratt and G. V. Raynor: *J. Inst. Met.*, 1951, vol. 79, p. 211.
19. I. Obinata and N. Komatsu: *Nippon Kinzoku Gakkai-Si*, 1955, vol. 19, p. 197.
20. G. Gustafsson, T. Thorvaldsson, and G. L. Dunlop: in "Metallurgy of Light Alloys", *Proc. Inst. of Metallurgists Conf.*, Loughborough, 1983, vol. 20, p. 288.
21. J. G. Barlock and L. F. Mondolfo: *Z. Metallkde*, 1975, vol. 66, p. 605.
22. D. Munson: *J. Inst. Met.*, 1967, vol. 95, p. 217.
23. H. Westengen: *Z. Metallkde*, 1982, vol. 73, p. 360.